

Optical properties of 3d transition-metal-doped MgAl₂O₄ spinels

K. Izumi,¹ S. Miyazaki,¹ S. Yoshida,¹ T. Mizokawa,² and E. Hanamura^{1,3}

¹*Chitose Institute of Science and Technology, 758-65 Bibi, Chitose, Hokkaido 066-8655, Japan*

²*Department of Physics and Department of Complexity Science and Engineering, University of Tokyo, 5-1-5 Kashiwanoha, Chiba 277-8561, Japan*

³*Japan Science and Technology Agency, 758-65, Bibi, Chitose, Hokkaido 066-8655, Japan*

(Received 15 March 2007; revised manuscript received 9 May 2007; published 10 August 2007)

Strong emission bands in the visible region are observed in MgAl₂O₄ crystals doped with transition-metal ions under excitation at the band-to-band transitions. We report optical responses of Cr-, Co-, and Ni-doped MgAl₂O₄ and present optical models for *M*-doped MgAl₂O₄ (*M*=Ti, V, Cr, Mn, Co, and Ni) to describe the charge-transfer transitions and the transitions between multiplet levels of 3d electrons, which are observed competitively or coexisting, depending on the number of 3d electrons. While the optical responses of Cr- and Ni-doped MgAl₂O₄ are dominated by the multiplet-multiplet transitions, those of Ti- and V-doped MgAl₂O₄ are governed by the charge-transfer transitions. The two kinds of transitions coexist in the Mn- and Co-doped MgAl₂O₄. These behaviors are well understood based on the numerical results of unrestricted Hartree-Fock approximation.

DOI: 10.1103/PhysRevB.76.075111

PACS number(s): 71.55.Ht, 71.20.Be

I. INTRODUCTION

Transition-metal *M* doped spinels *M*:MgAl₂O₄ (*M*=Ti, V, and Mn) were found to show strong emission and have been attracting much interest as a new laser material.¹ The spinel crystal MgAl₂O₄ belongs to the cubic space group *O_h* (*Fd3m*) with 8 f.u. per unit cell. One kind of octant contains a Mg²⁺ ion at the center and has a tetrahedral coordination of O²⁻ ions with full *T_d* symmetry (*A* site), and the other octant has a sixfold distorted octahedral coordination of Al³⁺, which is located at the position with *D_{3d}* symmetry (*B* site). The host MgAl₂O₄ itself may have various color centers due to Mg deficiency, Mg-Al antisite defect, etc.,^{2,3} that are affected by γ -ray,⁴ x-ray,⁵ and neutron⁶ irradiations. In the case of transition-metal-doped MgAl₂O₄, the interaction between the transition-metal (3d) levels and the defect levels of host MgAl₂O₄ affects the valency of the doped transition-metal ions. In addition, the doped transition-metal ions can substitute for *A*-site and/or *B*-site cations. For example, Fe:MgAl₂O₄ is dominated by *A*-site Fe²⁺ impurities^{7,8} although *B*-site Fe³⁺ can coexist in some natural spinels.^{9,10} These two points, namely, valency and site type of doped transition-metal *M* ions, are important in determining the optical responses of *M*-doped MgAl₂O₄.

The optical transitions in transition-metal-doped MgAl₂O₄ can be understood based on the ligand field theory.¹¹ For example, the red emission of Cr:MgAl₂O₄ was successfully interpreted as the transition from the lowest excited multiplet state ²*E_g* to the ground state multiplet ⁴*A_{2g}*,^{12,13} which is similar to that in the famous laser material Cr:Al₂O₃. Very recently, the Ti-doped spinel (Ti:MgAl₂O₄) was found to show strong blue emission under the band-to-band excitation, surprisingly in contrast to the red emission of Ti:Al₂O₃.¹⁴ The charge-transfer excitation plays a dominant role in the optical responses of Ti:MgAl₂O₄,¹⁴ while both the transitions between the multiplet levels and the charge-transfer transitions are observed to coexist in Mn:MgAl₂O₄.¹⁵ In order to understand the interplay of these two kinds of transitions, we have studied how optical re-

sponses of *M*-doped MgAl₂O₄ crystals (*M*=Ti, V, Cr, Mn, Co, and Ni) depend on the number of 3d electrons. In order to investigate the optical responses in a systematic way, it is very important to grow the *M*-doped MgAl₂O₄ crystals under the same condition since the optical properties of MgAl₂O₄ are sensitive to the various defects. Also it is important and interesting how the dependence of charge-transfer energy Δ and multiplet averaged Coulomb interaction *U* on the number of 3d electrons is related to the rich optical responses of *M*-doped MgAl₂O₄. These questions will be answered by the measurement of optical responses of the transition-metal-doped spinels with the help of calculations by unrestricted Hartree-Fock (UHF) approximation.

After a brief description of experimental and theoretical methods (Sec. II), we will show the optical spectra of Cr-, Co-, and Ni-doped spinels in Sec. III. Combined with the preceding results for Ti-,¹⁴ V-,¹⁶ and Mn-doped^{15,17} spinels, we will describe a systematic trend of optical responses of transition-metal-doped spinels. In Sec. IV, the systematic trend will be interpreted by optical models that are constructed based on the UHF calculations for transition-metal-doped spinels. Section V is devoted to discussion and conclusion.

II. EXPERIMENTAL AND THEORETICAL METHODS

The transition-metal-doped MgAl₂O₄ single crystals were grown from melt in an oxidizing atmosphere by the floating-zone method, with a Xe lamp as a heating source. Calcined powders of Al₂O₃ (99.999%) and MgO (99.99%) were used as starting materials. The nominal molar percentage of transition-metal doping is chosen from 0.01 to 1.0 mol % with the stoichiometric condition. Samples were sliced into a disk with a diameter of several millimeters and a thickness of 1.5 mm after being polished by diamond and alumina powders for optical measurements.

The valence of the transition-metal impurities and the position of the impurity level relative to the host O 2*p* band can be calculated by the UHF calculation on a spinel-type lattice

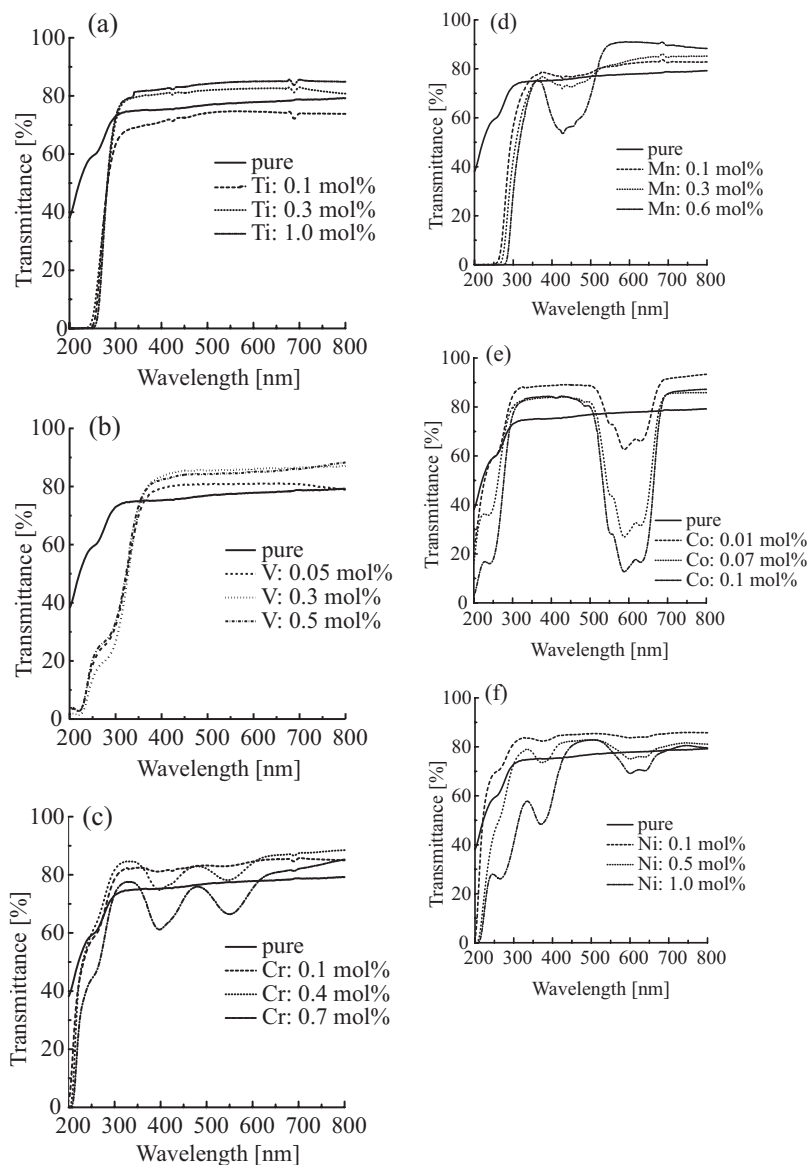


FIG. 1. Transmittance spectra of (a) Ti-, (b) V-, (c) Cr-, (d) Mn-, (e) Co-, and (f) Ni-doped MgAl_2O_4 crystals observed at room temperature.

model with eight *A*-site (Mg) ions, 16 *B*-site (Al) ions, and 32 oxygen ions in the unit cell. One of the *A*-site or *B*-site ions is replaced by the transition-metal impurity ion. The $3s$ orbitals of the *A*-site Mg and *B*-site Al ions, the $2p$ orbitals of the oxygen ions, and the $3d$ and $4s$ orbitals of the transition-metal ion are included in the model Hamiltonian. The transfer integrals between the atomic orbitals are given in terms of Slater-Koster parameters.¹⁸ The intra-atomic Coulomb interaction between the $3d$ electrons is expressed using Kanamori parameters, u , u' , j , and j' , and is treated by UHF approximation.¹⁹

III. OPTICAL RESPONSE

The transmission spectra of the transition-metal-doped spinels are summarized in Fig. 1. The thickness of the samples is fixed to 1.5 mm, and the doping degree is changed from 0.01 to 1.0 mol %. Here, only a few examples are shown in Fig. 1 in comparison with that of a pure MgAl_2O_4 crystal.

Several characteristics which will be discussed are listed here in reference to Fig. 1. Firstly, the absorption lines are induced in the visible region of Cr-, Mn-, Co-, and Ni-doped MgAl_2O_4 crystals, while any absorption lines are not visible in Ti- and V-doped spinels. Secondly, the absorption edge shows always the redshift due to the doping of the transition-metal ions. These characteristics as well as other optical responses will be explained well in Sec. IV by the model supplemented with the UHF calculations. Thirdly, the transmittance is also increased by doping in the spectral region, besides the frequency range of doping-induced absorption mentioned above. The transmittance of the pure MgAl_2O_4 crystals is degraded by the broad optical transitions due to Mg deficiency. In the case of Mn and Co doping, the transition-metal ions substitute for the *A*-site Mg ions and tend to reduce the Mg deficiency. Also for Cr and Ni doping, although the transition-metal ions mainly substitute for the *B*-site ions, some transition-metal ions may enter the *A* site and reduce the Mg deficiency. As for Ti and V doping, the Ti and V ions dominantly occupy the *B* site as Ti^{4+} and V^{5+} ,

and provide the 3d electron to the Mg deficiency. This charge compensation may result in the improvement of transmittance in the visible region.

The blue emission with its peak at 490 nm is observed under the band-to-band transition of Ti:MgAl₂O₄,¹⁴ while the blue-green emission around 505 nm is dominant in V:MgAl₂O₄.¹⁶ These were assigned to the charge-transfer deexcitation between the optically excited 3d electron and a hole created in the valence band. On the other hand, the red emission at 690 nm is dominantly observed in Cr:MgAl₂O₄ both under band-to-band excitation and pumping at two transmittance dips of 400 and 550 nm as shown in Figs. 2(a), 2(c), and 2(d). Figure 2(b) shows the excitation spectra monitored by the emission intensity at 687 nm. From these spectra, the red emission is assigned to the radiative decay from the lowest excited multiplet state ²E_g to the ground state multiplet ⁴A_{2g}. This assignment is consistent with that of the 700 nm emission observed in Cr:MgGa₂O₄.²⁰ The two dips at 550 and 400 nm in the transmittance spectrum, as shown in Fig. 1(c), are assigned to the excitation from the ground state multiplet ⁴A_{2g}, respectively, into ⁴T_{2g} and ⁴T_{1g} states of Cr³⁺ (3d)³ at B site.^{12,13,21}

The optical measurement of manganese-doped spinels Mn:MgAl₂O₄ was repeated by using the newly grown crystals. The same spectra as in Ref. 15 are obtained and the assignments are also confirmed. Only relevant results are repeated here. The green emission with its peak at 520 nm is assigned to the radiative decay from the lowest multiplet excited state ⁴T₁ into its ground state ⁶A₁ of Mn²⁺ (3d)⁵ at A (T_d) site. This assignment is confirmed by the excitation spectrum monitored by the emission at 520 nm; i.e., four peaks at 450, 425, 385, and 360 nm are assigned to the excitation from the ground state ⁶A₁, respectively, to ⁴T₂ (⁴G), ⁴A₁/⁴E (⁴G), ⁴T₂ (⁴D), and ⁴T₁ (⁴P)/⁴E (⁴D) of Mn²⁺ (3d)³ at A site. These excitations relax to the lowest excited multiplet state ⁴T₁ (⁴G) and emit 520 nm photon, making the transition to ⁶A₁. Also this assignment is consistent with that of the 500 nm emission observed in Mn:MgGa₂O₄.²² The red emission with its peak at 650 nm is assigned to the charge-transfer deexcitation due to the radiative recombination between one of the Mn²⁺ (3d)⁵ electron in ⁶A₁ multiplet ground state and the hole optically created in the valence band.

Cobalt-doped spinels Co:MgAl₂O₄ look very brilliantly blue under natural-light irradiation. Notice that the absorption coefficient at yellow around 600 nm of Co:MgAl₂O₄ is by 1 order of magnitude larger than those of the others shown in Fig. 1. The blue emission with its peak at 450 nm and red emission around 710 nm are observed under the band-to-band excitation, e.g., at 240 nm as shown in Figs. 3(a) and 3(b). As Figs. 3(c) and 3(d) show, the red emission with almost equal intensity is observed under the excitations at 626, 583, and 550 nm. The blue emission is assigned to the charge-transfer deexcitation between one of the Co²⁺ (3d)⁷ electrons at A site and a hole created in the valence band under the band-to-band excitation, while the red emission around 660 nm is assigned to the optical decay into the multiplet ground state ⁴A₂(⁴F) from the excited multiplet state ⁴T₁(⁴P). This assignment is consistent with that of the

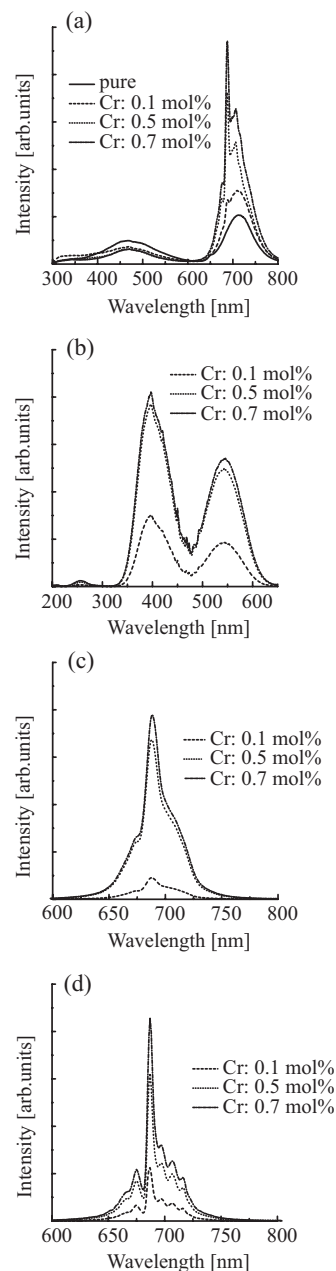


FIG. 2. Emission spectra of Cr-doped MgAl₂O₄ under excitation at (a) 244 nm, (c) 400 nm, and (d) 550 nm. (b) Excitation spectra monitored by the emission intensity at 687 nm.

650 nm emission observed in Co:MgGa₂O₄.²³ Three peaks in the excitation spectrum of Fig. 3(d) are assigned to the optical transitions from the ground state ⁴A₂(⁴F) into ²E/²T₁(²G, 626 nm), ⁴T₁(⁴P, 583 nm), and ²A₁/²T₂(²G, 550 nm), which are hybridized with each other by spin-orbit interaction. These excitations relax to the Stokes-shifted ⁴T₁(⁴P) and emit the radiation at 660 nm. These assignments are consistent with those of ligand field theory¹¹ and with the optical study by Kuleshov *et al.*²⁴ Here, the Co²⁺ (3d)⁷ ion is located at A site with T_d symmetry, so that these energy levels are described approximately in terms of the (3d)³ system in O_h site.¹¹ The ligand field theory²⁵ and cluster-model calculation²⁶ predict that the multiplet states

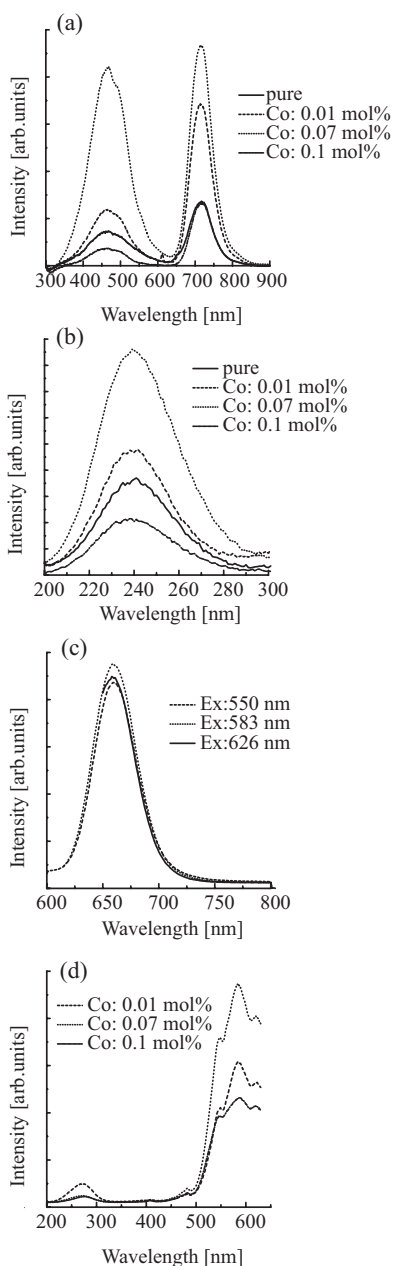


FIG. 3. (a) Emission spectra of Co:MgAl₂O₄ under excitation at 240 nm, and (c) those under excitation at three dips of the transmittance spectra of Fig. 1(e), i.e., 626, 583, and 550 nm. (b) Excitation spectra monitored at 450 nm and (d) those at 710 nm.

4T_1 and 4T_2 have much lower excitation energies 0.84 and 0.5 eV from the ground multiplet 4A_2 , so that these levels were not observed by our optical systems.

The electronic structure of Ni:MgAl₂O₄ crystal is described by Ni²⁺ ($3d$)⁸ levels at D_{3d} symmetry (B site), approximately at O_h symmetry. The ground multiplet state is ${}^3A_{2g}$ ($t_2^6e^2$), and the lowest excited state ${}^3T_{2g}$ ($t_2^5e^3$) has the excitation energy at ~ 1000 nm.^{27,28} The doublet structures at 640 and 590 nm in Fig. 1(f) are assigned to the excitation from ${}^3A_{2g}$ ($t_2^6e^2$) to 1E_g and ${}^3T_{1g}$ ($t_2^5e^3$), which are coupled by the spin-orbit interaction. Under the band-to-band excitation at 242 nm, the emission spectrum of blue-green with its peak

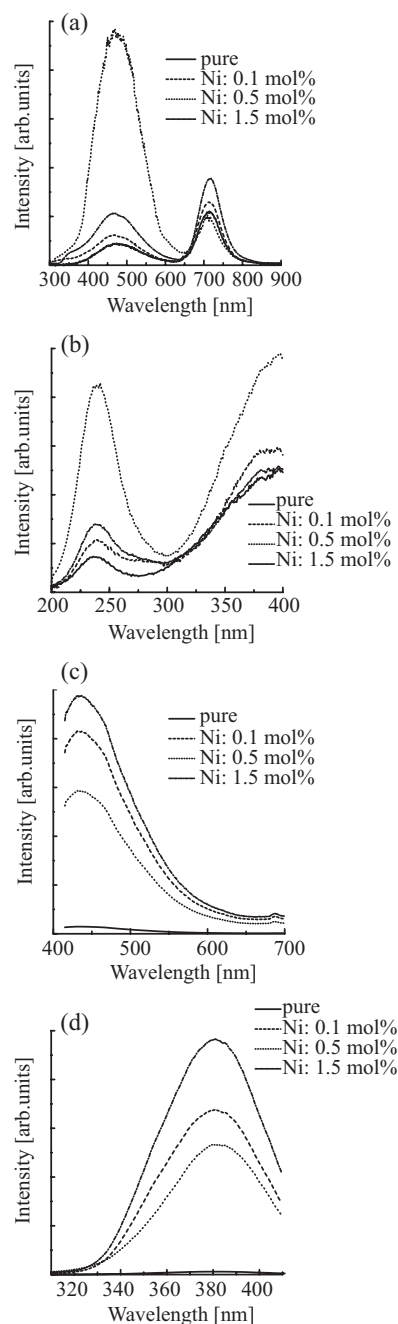


FIG. 4. (a) Emission spectra of Ni:MgAl₂O₄ under excitation at band edge at 242 nm, and (c) those under excitation at a dip (380 nm) of the transmittance spectra in Fig. 1(f). (b) Excitation spectra monitored by the emission intensity at 470 nm, and (d) those monitored by the emission intensity at 440 nm.

at 470 nm is observed as shown in Fig. 4(a), and its excitation spectrum is drawn in Fig. 4(b). The other blue emission with the peak at 440 nm is observed under pumping at 380 nm as shown in Fig. 4(c), and the excitation spectrum is drawn in Fig. 4(d).

IV. OPTICAL MODEL

In order to explain the rich optical responses of the transition-metal-doped spinels, optical models are con-

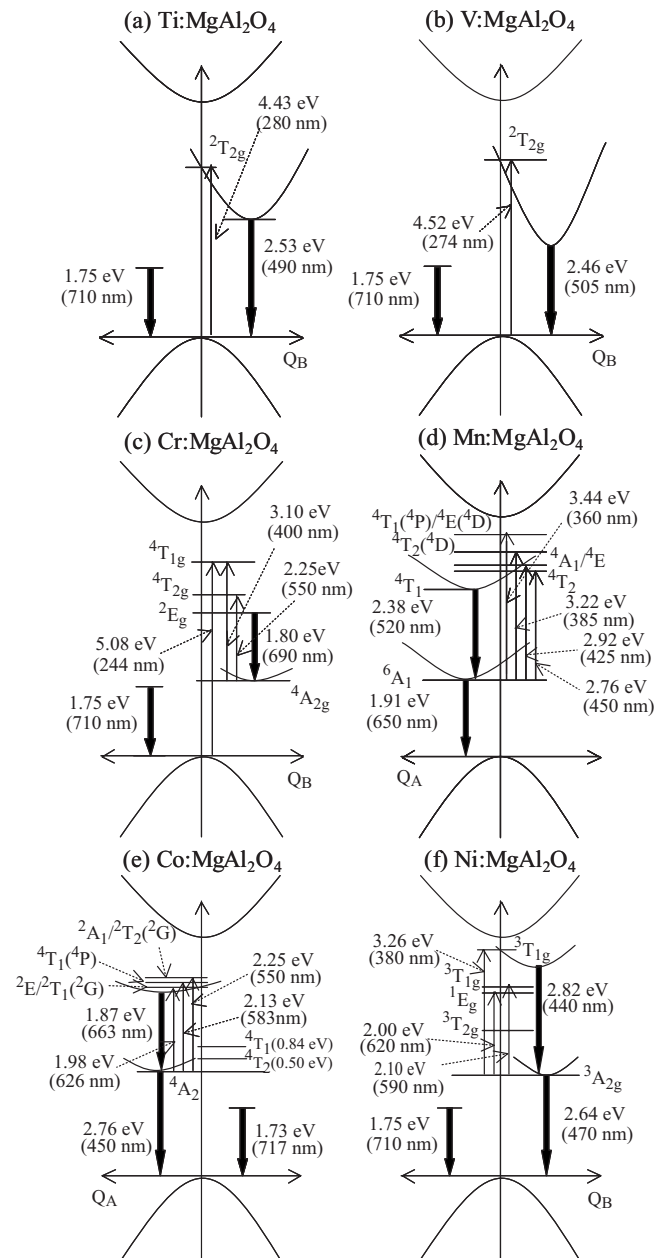


FIG. 5. Energy diagrams of MgAl_2O_4 crystals doped with (a) Ti, (b) V, (c) Cr, (d) Mn, (e) Co, and (f) Ni as a function of the interaction modes Q_A (at A site) and Q_B (at B site).

structured based on the UHF calculations. The first characteristics of the UHF calculation shows that $3d$ levels of the lighter transition-metals Ti and V, doped in MgAl_2O_4 crystal, are rather high. As a result, these $3d$ electrons are fully removed so that Ti and V exist as Ti^{4+} and V^{5+} at B site, losing all $3d$ electrons. These results are consistent with the models presented to understand the optical responses of Ti- and V-doped MgAl_2O_4 crystals.^{14,16} These are shown in Figs. 5(a) and 5(b), respectively.

It was also confirmed by electron spin resonance measurement that the titanium ion is located as Ti^{4+} at B site in the electronic ground state. The blue emission with its peak at 490 nm is assigned to the charge-transfer deexcitation of Ti^{3+} $3d$ into the valence band hole created

by the band-to-band excitation. The Stokes shift from 280 nm (4.43 eV) to 490 nm (2.53 eV) is of the same order of magnitude as that (500–800 nm) of $\text{Ti}:\text{Al}_2\text{O}_3$. The vanadium ion was also concluded to have a similar electronic structure, i.e., to exist as V^{5+} at B site in the electronic ground state as discussed in Ref. 16. The transmittance spectrum of $\text{V}:\text{MgAl}_2\text{O}_4$ crystal shows the largest redshift due to V doping, so that the conduction-band bottom is considered to be composed of the hybridized states of V^{4+} $3d$ and O^{2-} $2p$. Then bluish green emission with its peak at 505 nm is assigned to the radiative decay of V^{4+} $3d$ electron into the hole state in the valence band. Here, the Stokes shift from 274 nm (4.52 eV) to 505 nm (2.46 eV) is also of the same order of magnitude as Ti-doped MgAl_2O_4 and Al_2O_3 crystals. Both ions Ti^{3+} and V^{4+} are shown by the UHF calculation to lose the single $3d$ electron to the Mg deficiency. This compensation results in the improvement of transmittance in the visible region as shown in Figs. 1(a) and 1(b).

The multiplet-averaged Coulomb interaction U increases and the charge-transfer energy Δ decreases as the number of $3d$ electrons increases in going from Ti^{3+} ($3d^1$) to Cr^{3+} ($3d^3$). Therefore, the Cr^{3+} ($3d^3$) state is stable and the multiplet levels of Cr^{3+} electrons embedded at B site are shown to distribute within the band gap of MgAl_2O_4 crystal, in agreement with the optical responses discussed in Sec. III. The optical transitions between the multiplet levels are observed in the transmittance and emission (excitation) spectra and are assigned as shown in Fig. 5(c).

Manganese and cobalt are derived to exist as Mn^{2+} and Co^{2+} ions at A site, and the level schemata are well consistent with the observed optical spectra as shown in Figs. 5(d) and 5(e), respectively. Here, both the charge-transfer and multiplet levels can be fixed relative to the valence-band top. As to $\text{Mn}:\text{MgAl}_2\text{O}_4$, refer to Ref. 15. Here, we discuss the origin of brilliant blue of $\text{Co}:\text{MgAl}_2\text{O}_4$. There are three reasons for this enhancement. Firstly, the most important origin comes from the strong absorption at yellow (626, 583, and 550 nm), which is complementary to blue under natural white light irradiation. Secondly, the blue emission at 450 nm is induced by the charge-transfer deexcitation due to the radiative recombination of one of the Co^{2+} ($3d^7$) electrons and the hole optically created in the valence band under the band-to-band excitation around 240 nm. Thirdly, the transmittance in the blue region increases by more than 10%, so that the blue light becomes more transparent in $\text{Co}:\text{MgAl}_2\text{O}_4$ crystal. These three effects result in the more brilliant blue than other cobalt blue. Taking into account the Co^{2+} ($3d^7$) electrons in T_d symmetry, the electronic structure of $\text{Co}^{2+}:\text{MgAl}_2\text{O}_4$ is given in Fig. 5(e). Note here that these levels are similar to those of the ($3d^3$) electrons in O_h crystalline field, with the Dq value reduced by 5/9.¹¹ The triplet structures in Fig. 1(e) are ${}^2E/{}^2T_1({}^2G, 626 \text{ nm})$, ${}^4T_1({}^4P, 583 \text{ nm})$, and ${}^2A_1/{}^2T_2({}^2G, 550 \text{ nm})$, which are well hybridized by the spin-orbit interaction. These excitations relax to the lattice-distorted level of ${}^2E/{}^2T_1$ and show the emission with peak at 663 nm. On the other hand, under the band-to-band excitation, the blue emission at 450 nm is assigned to the radiative recombination of a hole created at the valence band with an electron composing the ground state multiplet of Co^{2+} ($3d^7$).

The electronic structure and optical responses of Ni:MgAl₂O₄ crystals are also understood in the way similar to that of Co:MgAl₂O₄. Here, Ni ion is assigned to Ni²⁺ (3d)⁸ in *B* site with *O_h* symmetry. Then the electronic structure of Ni:MgAl₂O₄ is drawn in Fig. 5(f). Here, the blue emission at 440 nm is assigned to the transition from the multiplet state ³T_{1g} (*t_{2g}⁴e⁴*) to the ground state multiplet ³A_{2g} (*t_{2g}⁶e²*), while under the band-to-band excitation, the charge-transfer deexcitation is due to the recombination of a hole created in the valence band with one of the (3d)⁸ electrons on ³A_{2g} (*t_{2g}⁶e²*). This is also drawn in Fig. 5(f).

V. DISCUSSION

As a conclusion, almost all optical characteristics of transition-metal-doped spinel Ti:, V:, Cr:, Mn:, Co:, and Ni:MgAl₂O₄ crystals are discussed from a unified point of view in the framework of the UHF approximation. Notice that Mn²⁺ (3d)⁵ and Co²⁺ (3d)⁷ are located at the *A* site replacing Mg²⁺ ion, while Ti⁴⁺ and V⁵⁺ as well as Cr³⁺ (3d)³ and Ni²⁺ (3d)⁸ are at the *B* site replacing Al³⁺ ion. The systematic trend of valency and charge-transfer energy has been well understood by the UHF calculations. Unfortunately, however, we could not observe the low-lying energy levels beyond 900 nm by our optical systems, so that level assignment of Co and Ni was restricted to the visible region. The infrared spectroscopy will be able to check the low-lying

levels which have been assumed in the present paper.

The most important characteristics of transition-metal-doped spinels is the coexistence of charge-transfer excitation and optical transition between the multiplet states of (3d)^{*n*} electrons in the visible region. In the case of Ti- and V-doped MgAl₂O₄ crystal, only the charge-transfer excitation between the optically excited 3d electron and the hole created in the valence band is observed in the visible region. This is because all 3d electrons of Ti and V atoms are removed and the 3d orbitals and 2p orbitals of O²⁻ (2p)⁶ are well hybridized. On the other hand, both transitions are clearly visible in Co- and Mn-doped MgAl₂O₄ crystals because the multiplet terms of (3d)⁷ and (3d)⁵ are distributed in the band gap. It is also noted here that both Co²⁺ and Mn²⁺ ions are at the *A* site with *T_d* symmetry, without the inversion symmetry, so that the multiplet transitions have rather large oscillator strength. In Cr- and Ni-doped spinels, the transitions between the multiplet terms are dominant and the charge-transfer transition is rather weak. Here, both ions Cr³⁺ and Ni²⁺ are at the *B* site.

ACKNOWLEDGMENTS

The authors would like to acknowledge the fruitful discussions with Y. Tanabe, Y. Kawabe, and A. Yamanaka. This work was supported by a Grant-In-Aid for Scientific Research from the Ministry of Education, Culture, Sports, Science and Technology of Japan.

-
- ¹E. Hanamura, Y. Kawabe, H. Takashima, T. Sato, and A. Tomita, *J. Nonlinear Opt. Phys. Mater.* **12**, 467 (2003).
²D. Bacorisen, R. Smith, B. P. Uberuaga, K. E. Sickafus, and J. A. Ball, *Phys. Rev. B* **74**, 214105 (2006).
³B. P. Uberuaga, D. Bacorisen, R. Smith, J. A. Ball, R. W. Grimes, A. F. Voter, and K. E. Sickafus, *Phys. Rev. B* **75**, 104116 (2007).
⁴G. P. Summers, G. S. White, K. H. Lee, and J. H. Crawford, Jr., *Phys. Rev. B* **21**, 2578 (1980).
⁵A. Ibarra, F. J. López, and M. Jiménez de Castro, *Phys. Rev. B* **44**, 7256 (1991).
⁶L. S. Cain, G. J. Pogatschnik, and Y. Chen, *Phys. Rev. B* **37**, 2645 (1988).
⁷G. A. Slack, F. S. Ham, and R. M. Chrenko, *Phys. Rev.* **152**, 376 (1966).
⁸E. S. Gaffney, *Phys. Rev. B* **8**, 3484 (1973).
⁹A. D. Giusta, S. Carbonin, and G. Ottonello, *Miner. Mag.* **60**, 603 (1996).
¹⁰T. N. Michail and M. Koch-Müller, *Phys. Chem. Miner.* **32**, 175 (2005).
¹¹H. Kamimura, S. Sugano, and Y. Tanabe, *Ligand Field Theory and Its Applications* (Syokabo, Tokyo, 1969), in Japanese; S. Sugano, Y. Tanabe, and H. Kamimura, *Multiplets of Transition Metal Ions in Crystals* (Academic, New York, 1970).
¹²D. L. Wood, G. F. Imbusch, R. M. Macfarlane, P. Kisliuk, and D. M. Larkin, *J. Chem. Phys.* **48**, 5255 (1968).
¹³F. H. Lou and D. W. G. Ballentyne, *J. Phys. C* **1**, 608 (1968).
¹⁴T. Sato, M. Shirai, K. Tanaka, Y. Kawabe, and E. Hanamura, *J. Lumin.* **114**, 155 (2005).
¹⁵A. Tomita, T. Sato, K. Tanaka, Y. Kawabe, M. Shirai, and E. Hanamura, *J. Lumin.* **109**, 19 (2004).
¹⁶Y. Fujimoto, H. Tanno, A. Yamanaka, Y. Kawabe, and E. Hanamura (unpublished).
¹⁷H. Kudo, M. Kitaya, H. Kobayashi, M. Shirai, K. Tanaka, Y. Kawabe, and E. Hanamura, *J. Phys. Soc. Jpn.* **75**, 014708 (2006).
¹⁸W. A. Harrison, *Electronic Structure and the Properties of Solid* (Dover, New York, 1989).
¹⁹T. Mizokawa and A. Fujimori, *Phys. Rev. B* **54**, 5368 (1996).
²⁰L. P. Sosman, T. Abritta, O. Nakamura, and M. M. F. D'Auiar Neto, *Phys. Status Solidi A* **147**, K107 (1995).
²¹C. Garapon, A. Brenier, and R. Moncorge, *Opt. Mater. (Amsterdam, Neth.)* **10**, 177 (1998).
²²T. K. Tran, W. Park, J. W. Tomm, B. K. Wagner, S. M. Jacobsen, C. J. Summers, P. N. Yocom, and S. K. McClelland, *J. Appl. Phys.* **78**, 5691 (1995).
²³L. P. Sosman and T. Abritta, *Solid State Commun.* **82**, 801 (1992).
²⁴N. V. Kuleshov, V. P. Mikhailov, V. G. Shcherbitsky, P. V. Prokoshin, and K. V. Yumashev, *J. Lumin.* **55**, 265 (1993).
²⁵A. Fazzio, M. J. Caldas, and A. Zunger, *Phys. Rev. B* **30**, 3430 (1984).
²⁶T. Mizokawa and A. Fujimori, *Phys. Rev. B* **48**, 14150 (1993).
²⁷N. V. Kuleshov, V. G. Shcherbitsky, V. P. Mikhailov, S. Kück, J. Koetke, K. Petermann, and G. Huber, *J. Lumin.* **71**, 265 (1997).
²⁸T. Suzuki, G. S. Murugan, and Y. Ohishi, *J. Lumin.* **113**, 265 (2005).